PROCEEDINGS OF SCIENCE

Where on the Earth's surface are the biggest changes in cosmic ray intensity during geomagnetic storms?

Daniel Gecášek,[a,*] **Viacheslav Mykhailenko,**[b] **Pavol Bobík,**[c] **Ján Villim**[a] **and Ján Genči**[a]

[a] *Technical University of Košice, Department of computers and informatics, Letná 9, Košice, Slovakia*

[b] *P. J. Safarik University, Institute of Physics, Faculty of Science, Park Angelinum 9, Košice, Slovakia*

[c] *Institute of Experimental Physics, Slovak Academy of Sciences, Watsonova 47, Košice, Slovakia*

E-mail: daniel.gecasek@tuke.sk, slava@saske.sk, bobik@saske.sk, jan.villim@student.tuke.sk, jan.genci@tuke.sk

The geographical distribution of cosmic ray intensity at the Earth's surface significantly changes, mostly with geomagnetic latitude. Moreover, the transparency of the magnetosphere changes temporally, with significant changes during geomagnetic storms. In this article, we address the question: Where on the Earth's surface are the biggest relative and absolute changes in cosmic ray intensity during geomagnetic storms? We simulate a global situation for a set of selected geomagnetic storms and discuss obtained results.

38th International Cosmic Ray Conference (ICRC2023)
26 July - 3 August, 2023
Nagoya, Japan

*Speaker

PoS(ICRC2023)101

1. Introduction

The evolution of cut-off rigidities during geomagnetic storms has been presented in many papers. Usually, the method for backtracing particles is used and the situation for several positions on Earth, most typically neutron monitor positions is evaluated [1–3]. There is also research evaluating cut-off rigidities globally presented in [4] for one selected moment, where the changes in cut-off rigidities are evaluated from the difference of cut-off rigidities in combined internal and external geomagnetic fields and rigidities evaluated only in the internal geomagnetic field.

In this article, we aim to employ the capabilities of the COR system [5] to provide huge simulations of particle trajectories in Earth's magnetosphere, in order to evaluate the time evolution of cut-off rigidities on an hourly basis for two strong geomagnetic storms for the entire Earth's surface. Following this, we use these results to evaluate where on the Earth the effect of magnetosphere transparency to cosmic ray (CR hereafter) intensity is biggest.

2. Cut-off rigidities and CR intensities during selected geomagnetic storms

To quantify global changes in CR intensities at the top of the atmosphere during magnetic storms, we selected two relatively strong magnetic storms from March 2015 and December 2015. The selection criteria include the strength of the geomagnetic storm, the presence of clear storm patterns in neutron monitors data, and input data availability for geomagnetic models used. The resulting simulations evaluate the vertical approach of cosmic rays to the top of the atmosphere for a net of points covering the entire Earth's surface with a 5-degree step in latitude and longitude. This was done for both storms in hourly steps, specifically the following intervals were evaluated: the period between 2015-03-17 04:00:00 and 2015-03-20 00:00:00 for the first storm, and the period between 2015-12-19 00:00:00 and 2015-12-25 00:00:00 for the second storm.

For both simulations, the IGRF model [6] of the internal geomagnetic field, in combination with the Tsyganenko-Sitnov 05 model [7] of the external geomagnetic field were used. For the spectrum at the edge of the Earth's magnetosphere (at the magnetopause) we used the Force field spectrum from [8, 9]. The simulations contain the evaluation of trajectories for 72x37 geographical locations for 69 times (183816 simulations) for the March storm, and 72x37 geolocations x 145 hours (386280 simulations) for the December storm.

The Dst index [10] for March 2015 (dashed blue line) and December 2015 (solid orange line) is presented in figure 1. The first geomagnetic storm started on March 17 2015, and the Dst index reached a minimum value of -234 nT at 23:00 UTC. The second geomagnetic storm started on December 20 2015, and the Dst index reached a minimum value of -166 nT at 23:00 UTC.

The example of evaluated effective cut-off rigidities [11] for five points at the northern hemisphere with geographical longitude 40° and latitudes 40°, 45°, 50°, 55°, and 60°, is presented in figure 2. Time evolution of effective cut-off rigidities starts a few hours before the geomagnetic storm reaches Earth, and lasts until the recovery phase of the storm, which is shown. The evolution of cut-off rigidities during a storm has a characteristic pattern with decreasing values of cut-off rigidities during the first phase of the storm followed by the recovery phase with increasing rigidities. For example, for positions with longitude 40° and latitude 55°, effective cut-off rigidity decreased from values over 2 GV before the storm, to values less than 1.4GV during a maximum of the storm.

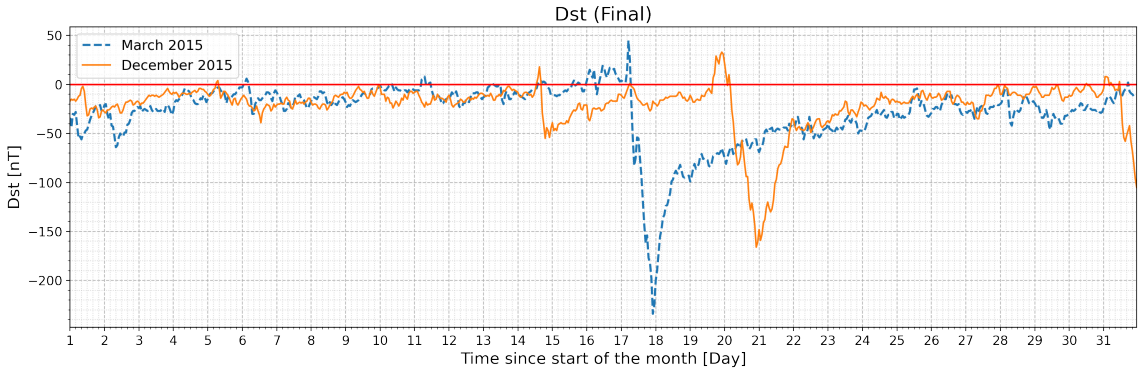

Figure 1: Dst index for March and December of 2015. Sources: https://wdc.kugi.kyoto-u.ac.jp/dst_final/201503/ and https://wdc.kugi.kyoto-u.ac.jp/dst_final/201512/

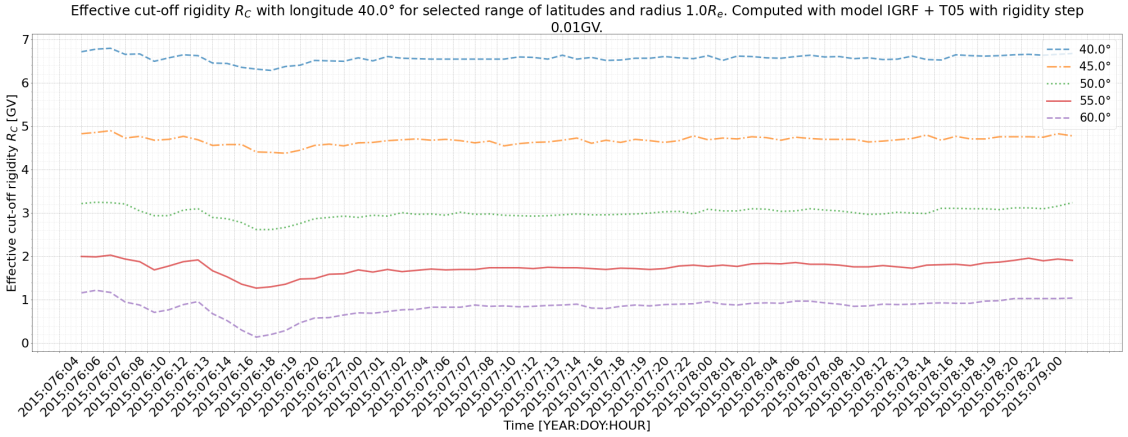

Figure 2: Example of evaluated effective cut-off rigidities during a geomagnetic storm in March 2015, for five points at north hemisphere with geographical longitude 40° and latitudes 40°, 45°, 50°, 55°, and 60°.

With the simulated trajectories described above, we could evaluate intensities at the top of the atmosphere from evaluated spectra of allowed and forbidden rigidities. The resulting intensities for the same selected points at longitude 40° are shown in figure 3.

2.1 Global analysis of the March 2015 geomagnetic storm

In figure 4 the average intensity value of the whole simulated grid is shown in the foreground, and the Dst index for the same time period in the background. Intensities are evaluated for am energy range between 0.01GV and 100GV. Let us note that this evolution comes from a change of magnetosphere transparency. The outer spectrum at the edge of the magnetopause, taken from Force field, changes only as a linear approximation between published values with month time step in [9]. Force field with monthly steps averages storm values to whole month values, thus spectra stay constant during the month and linear approximation does not improve the situation significantly. Hence, outer spectrum evolution during the storm is not part of the estimation presented in figure 3.

In figure 4, red dots signify hours when extreme values of global average cosmic ray intensity occur. The trend of the intensity plot roughly anticorrelates with the Dst trend, but there are some

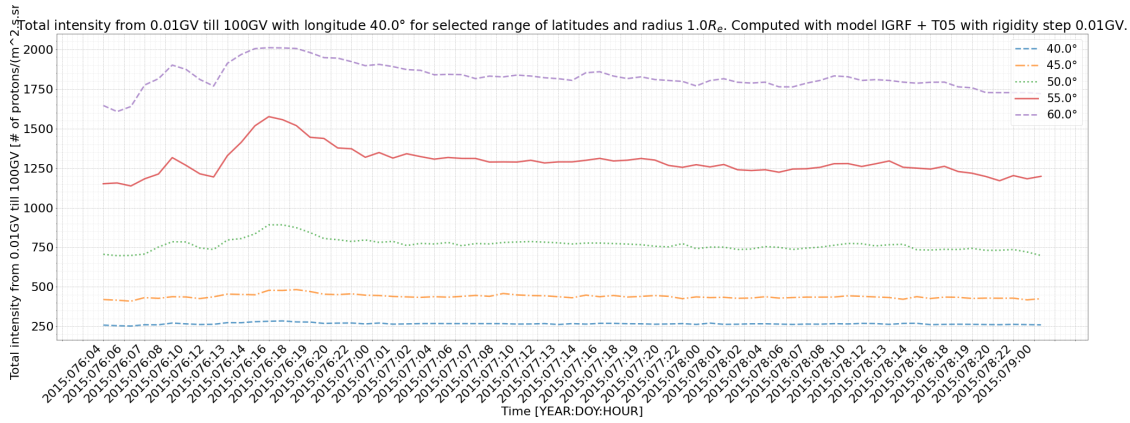

Figure 3: Cosmic ray intensity at the Earth's surface (top of the atmosphere), predicted by model with Force field spectrum, for longitude 40° and five selected latitudes at the north hemisphere.

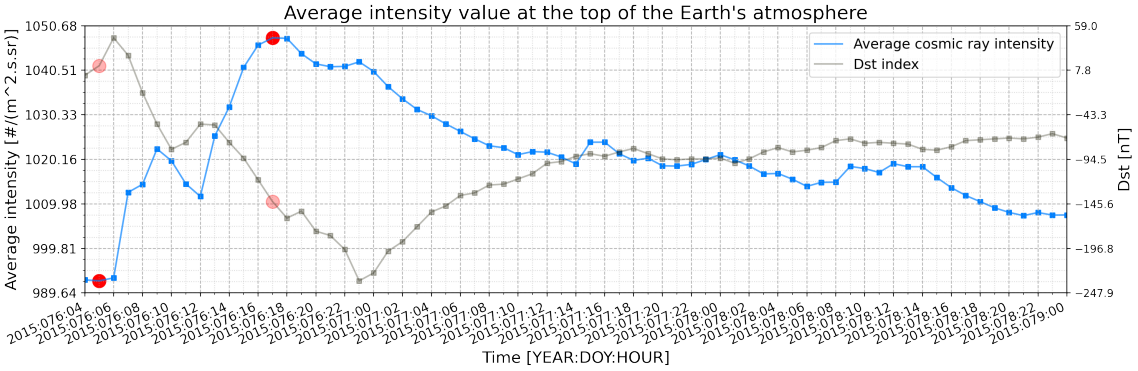

Figure 4: Average global cosmic ray intensity at the top of the Earth's atmosphere, and Dst index for March 2015 storm. The red points signify minimum and maximum values of average global cosmic ray intensity.

differences. For example, the smallest intensity does not occur at the same time as the greatest Dst value, but an hour before. Similarly, the greatest average global CR intensity does not coincide with the Dst minimum, but occurs 6 hours before Dst reaches its minimum.

Generally, for the March 2015 storm, the transparency of the magnetosphere globally allows over 5 percent more particles (only protons with energies in range 0.01GV to 100GV are considered) to reach the top of the atmosphere in the maximum moment of the storm, compared with intensities before the storm.

In figure 5 a map of relative differences of CR intensities for the March 2015 storm, between times with the greatest difference of global CR intensities (signified by the red dots in figure 4), is shown. Overall, the intensity increased on most of the globe, and it only decreased on less than 0.01% of the Earth's area, mostly in the polar regions. The median relative CR intensity increase was 2.36%, and the mean increase was 5.39%. The greatest changes can be seen in middle latitudes of both hemispheres. This region extends to a part of the South Atlantic Anomaly. Besides that, there is a region of slight increase between 135° West and 45° East in the equatorial region (crossing the prime meridian).

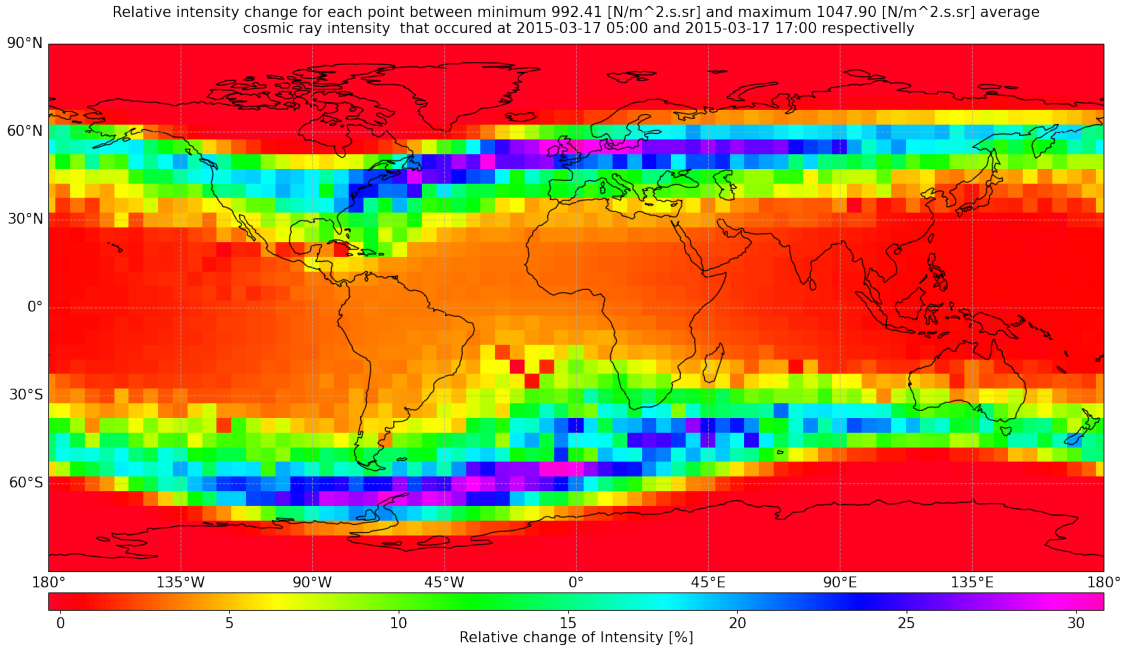

Figure 5: Relative CR intensity at the top of the Earth's atmosphere for each evaluated point between times with minimum and maximum average intensity signified by red dots in figure 4.

Table 1: Statistical parameters of global distribution of CR intensities between moments with maximum and minimum global intensity during two geomagnetic storms.

Statistical Parameters of global distribution of CR intensities between minimum and maximum global CR intensity	Geomagnetic Storms	
	17 March 2015	19 December 2015
Median CR intensity change	2.36%	1.67%
Average CR intensity change	5.39%	4.34%
Earth's area where CR intensity decreased	0.757%	0.725%
Median CR intensity decrease	-0.00149%	-0.00119%
Average CR intensity decrease	-0.01009%	-0.88407%

Statistical parameters describing the global distribution of CR intensities are summarized in Table 1. Parameters are evaluated between distributions of evaluated intensities in moments when global intensity was minimal and maximal during the storm.

2.2 Global analysis of the December 2015 geomagnetic storm

In figure 6, the average intensity value of the whole simulated grid is shown in the foreground, and the Dst index for the same time period in the background. The red dots signify moments when extreme values of global average CR intensity occur. Similarly, as was the case with the previous storm, the trend of the intensity plot roughly anticorrelates with the Dst trend but there are some differences. For example, the lowest intensity does not occur at the same time as the greatest Dst value, but 3 hours before that. Similarly, the greatest average global CR intensity does not coincide with the Dst minimum, but occurs 4 hours before Dst reaches its minimum.

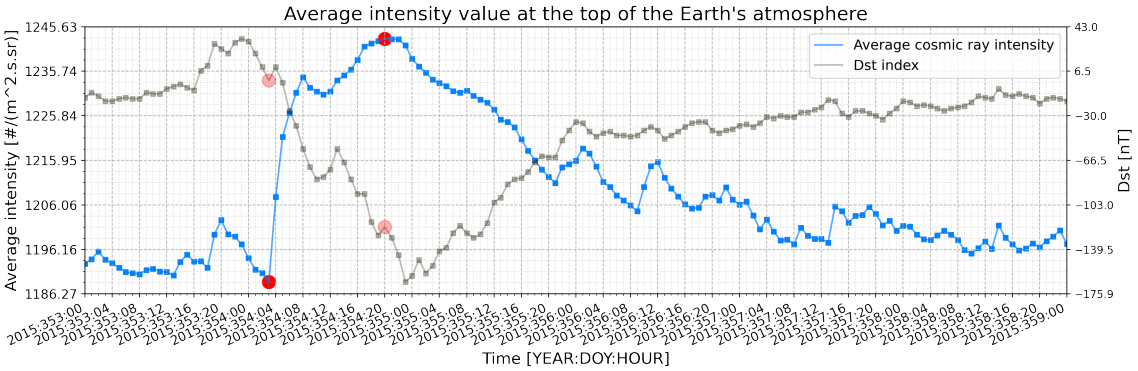

Figure 6: Average global CR intensity at the top of the Earth's atmosphere, and Dst index for December 2015 storm. The red points signify minimum and maximum values of average global CR intensity.

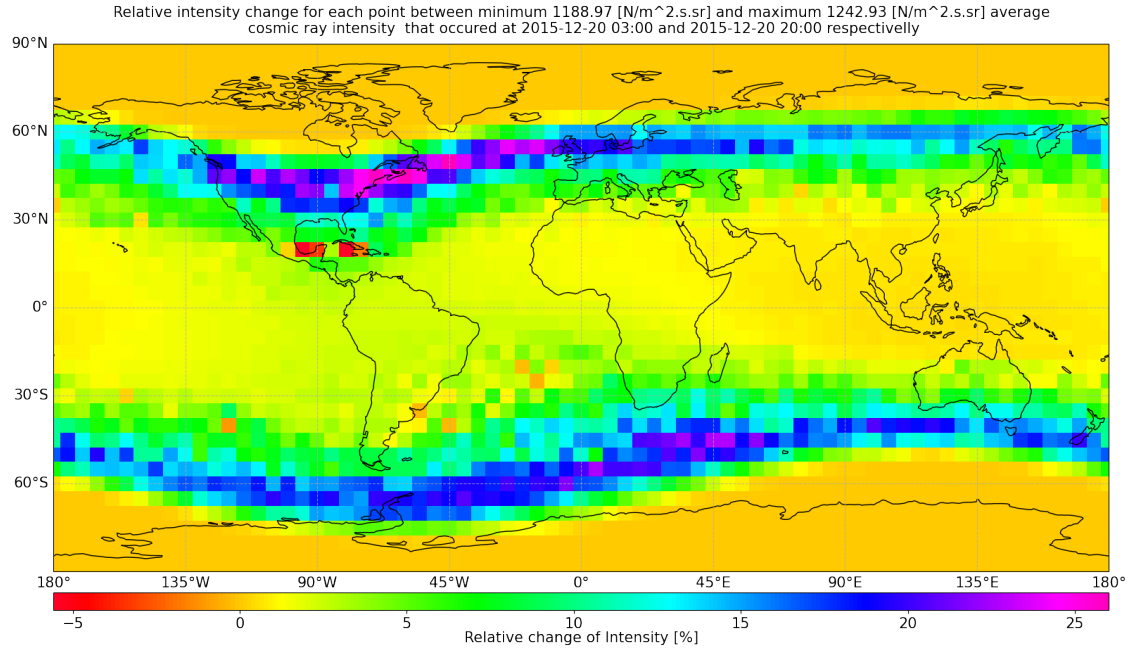

Figure 7: Relative CR intensity at the top of the Earth's atmosphere for each evaluated point between time-points with minimum and maximum average intensity signified by red dots in the figure 6.

In figure 7 a map of a relative differences of CR intensities for the December 2015 storm, between times with the greatest difference of global CR intensities (signified by red dots in figure 6), is shown. Overall, the intensity has increased on most of the globe, and it only decreased on less than 1% of the Earth's area, in the polar regions and some equatorial regions near Yucatan peninsula and Cuba. The median relative CR intensity increase was 1.67%, and the mean increase was 4.34%. The greatest changes can be seen in middle latitudes of both hemispheres. This region extends to a part of the South Atlantic Anomaly. Besides that, there is a region of slight CR increase between 135° West and the prime meridian in the equatorial region. Statistical parameters describing the global distribution of CR intensities are summarized in Table 1.

3. Discussion

As figures 4 and 6 show, intensities from COR simulation rise during geomagnetic storms. Because cut-off rigidities decrease, transparency of the magnetosphere increases and evaluated intensities during the storm are higher. The presented results show a situation when the spectrum entering the magnetosphere does not change during the geomagnetic storm. The Force field spectrum used in this simulation is provided in months, i.e. COR uses linear interpolation between values between from mid-March (in the case of the first storm) or mid-December (in the case of the second one), and the previous or following month values. The intensity at the Earth's top of atmosphere predicted by the model with Force field spectrum will, as one could expect, increase, as shown in figure 3.

This is the opposite of a measured situation, provided for example by neutron monitors. To solve this, the spectrum entering the magnetosphere must be described on a shorter time scale than the monthly spectra provided by the Force field approximation used. The expected pattern is that intensities of external spectra using shorter time steps will decrease during the storm. This could be concluded from the evolution of intensities in neutron monitor measurements from stations with low cut-off rigidity, i.e. those where the effect of the magnetosphere is small. Another option are spectra on a daily or shorter time base measured by orbital experiments with event selection, where the effect of the magnetosphere is not included. There is only one experiment currently offering such spectra in the range of energies where solar modulation play a role, and that is AMS-02. In future research, AMS-02 daily spectra [12] and daily Force field spectra [13] will be applied.

4. Conclusion

We evaluated CR intensities at the top of the Earth's atmosphere for two geomagnetic storms, the first in March 2015 and the second in December 2015. Although both storms had similar evolution, the March storm caused greater intensity increases due to changed magnetosphere transparency. This is consistent with a greater Dst decrease of the March storm.

In both storms, the greatest relative CR intensity increases due to magnetosphere transparency occurred in regions located on the polar edges of middle latitudes. More specificlly, those locations are the southern part of Northern Europe, and northern parts of the Southern Ocean near the Antarctic peninsula in the March storm, and the northeastern part of the USA, and southern Indian Ocean in the case of the December storm.

Relative CR intensity changed very little in the polar regions and a little more in equatorial regions. In both storms, the greatest relative change near the equator occurred within the same longitudes as the greatest relative change in the middle latitudes (near the Atlantic Ocean in the March 2015 storm, and South America in the December 2015 storm).

5. Acknowledgement

This work was supported by the TUKE Space Forum ESA PECS project. We thank Jakub Ulík for proofreading.

References

[1] K. Kudela, R. Bučik and P. Bobik, *On transmissivity of low energy cosmic rays in disturbed magnetosphere*, *Advances in Space Research* **42** (2008) 1300.

[2] M. Tyasto, O. Danilova, N. Ptitsyna and V. Sdobnov, *Variations in cosmic ray cutoff rigidities during the great geomagnetic storm of november 2004*, *Advances in Space Research* **51** (2013) 1230.

[3] M. Kravtsova and V. Sdobnov, *Cosmic rays during great geomagnetic storms in cycle 23 of solar activity*, *Geomagnetism and Aeronomy* **56** (2016) 143.

[4] O. Danilova, I. Demina, N. Ptitsyna and M. Tyasto, *Mapping of geomagnetic cutoff rigidity of cosmic rays during the main phase of the magnetic storm of november 20, 2003*, *Geomagnetism and Aeronomy* **59** (2019) 147.

[5] D. Gecášek, P. Bobík, J. Genči, J. Villim and M. Vaško, *Cor system: A tool to evaluate cosmic ray trajectories in the earth's magnetosphere*, *Advances in Space Research* **70** (2022) 1153.

[6] C. Finlay, E. Thbault and H. Toh, *Special issue "international geomagnetic reference field-the twelfth generation*, *Earth, Planets and Space* **67** (2015) 158.

[7] N.A. Tsyganenko and M.I. Sitnov, *Modeling the dynamics of the inner magnetosphere during strong geomagnetic storms*, *Journal of Geophysical Research: Space Physics* **110** (2005) A03208.

[8] R. Vainio, L. Desorgher, D. Heynderickx, M. Storini, E. Flückiger, R.B. Horne et al., *Dynamics of the earth's particle radiation environment*, *Space science reviews* **147** (2009) 187.

[9] I.G. Usoskin, A. Gil, G.A. Kovaltsov, A.L. Mishev and V.V. Mikhailov, *Heliospheric modulation of cosmic rays during the neutron monitor era: Calibration using pamela data for 2006–2010*, *Journal of Geophysical Research: Space Physics* **122** (2017) 3875.

[10] M. Nose, T. Iyemori, M. Sugiura and T. Kamei, "Geomagnetic dst index." World data center for geomagnetism, 10.17593/14515-74000, 2015.

[11] D. Cooke, J. Humble, M. Shea, D. Smart, N. Lund, I. Rasmussen et al., *On cosmic-ray cut-off terminology*, *Il Nuovo Cimento C* **14** (1991) 213.

[12] M. Aguilar, L.A. Cavasonza, G. Ambrosi, L. Arruda, N. Attig, F. Barao et al., *Periodicities in the daily proton fluxes from 2011 to 2019 measured by the alpha magnetic spectrometer on the international space station from 1 to 100 gv*, *Physical review letters* **127** (2021) 271102.

[13] P. Väisänen, I. Usoskin, R. Kähkönen, S. Koldobskiy and K. Mursula, *Revised reconstruction of the heliospheric modulation potential for 1964–2022*, *Journal of Geophysical Research: Space Physics* (2023) e2023JA031352.